ISBN: 978-3-95450-217-2 doi:10.18429/JACoW-ERL2019-TUCOXBS04

THE LHeC ERL – OPTICS AND PERFORMANCE OPTIMIZATION*

S.A. Bogacz†, Jefferson Lab, Newport News, VA, USA

Abstract

Unprecedently high luminosity of 10^{34} $cm^{-2}s^{-1}$, promised by the LHeC accelerator complex poses several beam dynamics and lattice design challenges [1]. Here we present beam dynamics driven approach to accelerator design, which in particular, addresses emittance dilution due to quantum excitations and beam breakup instability in a large scale, multi-pass Energy Recovery Linac (ERL) [2]. The use of ERL accelerator technology to provide improved beam quality and higher brightness continues to be the subject of active community interest and active accelerator development of future Electron Ion Colliders (EIC). Here, we employ current state of though for ERLs aiming at the energy frontier EIC. The main thrust of these studies was to enhance the collider performance, while limiting overall power consumption through exploring interplay between emittance preservation and efficiencies promised by the ERL technology [3].

ERL ARCHITECTURE

The ERL layout is sketched in Fig. 1. The machine is arranged in a racetrack configuration hosting two superconducting linacs in the parallel straights and three recirculating arcs on each side. The linacs are 1 km long and the arcs have 1 km radius, additional space is taken up by utilities like spreading, matching and compensating sections. The total length is 9 km: 1/3 of the LHC circumference. Each of the two linacs provides 10 GV accelerating field, therefore a 60 GeV energy is achieved in three turns. After the collision with the protons in the LHC, the beam is decelerated in the three subsequent turns. The injection and dump energy has been chosen at 500 MeV.

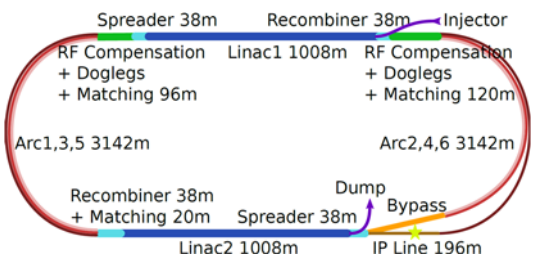

Figure 1: Scheme of the LHeC ERL layout.

Linac Design and Optimization

Each 1 km long linac hosts 72 cryo-modules, each containing 8 cavities for a total of 576 cavities per linac operating at 802 MHz. In the baseline design a quadrupole is placed every two cryomodules providing a FODO configuration. Note that the optics of a high gradient linac can be substantially perturbed by the additional focusing coming from the RF [4]. It is therefore important to make sure that it is properly modelled.

Energy recovery in a racetrack topology explicitly requires that both the accelerating and decelerating beams share the individual return arcs. This in turn, imposes specific requirements for TWISS function at the linacs ends: the TWISS functions have to be identical for both the accelerating and decelerating linac passes converging to the same energy and therefore entering the same arc.

To visualize beta functions for multiple accelerating and decelerating passes through a given linac, it is convenient to reverse the linac direction for all decelerating passes and string them together with the interleaved accelerating passes, as illustrated in Fig. 2. This way, the corresponding accelerating and decelerating passes are joined together at the arcs entrance/exit. Therefore, the matching conditions are automatically built into the resulting multi-pass linac beamline.

The optics of the two linacs are symmetric, the first being matched to the first accelerating passage and the second to the last decelerating one. In order to maximize the BBU threshold current, the optics is tuned so that the integral: is minimized. The resulting phase advance per cell is close to 130°. Non-linear strength profiles and more refined merit functions were tested, but they only brought negligible improvements.

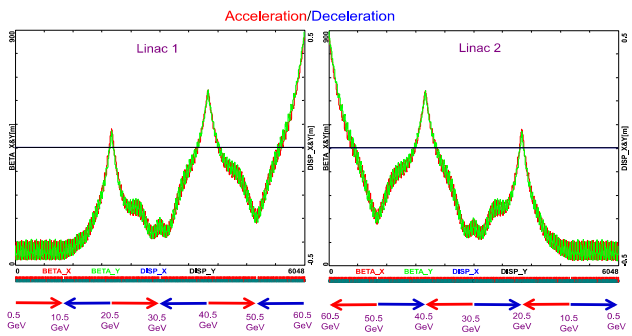

Figure 2: Beta function in the optimized LHeC Linacs during the acceleration. The linac contains 576 cavities.

Recirculating Arcs

All six arcs (three on each side) are accommodated in a tunnel of 1 km radius. Their lattice cell adopts a flexible momentum compaction layout that presents the very same footprint for each arc. This allows us to stack magnets on top of each other or to combine them in a single design. The dipole filling factor of the cell is 76%; therefore, the effective bending radius is 760 m.

The tuning of each arc takes into account the impact of synchrotron radiation at different energies. At the highest

* Work has been authored by Jefferson Science Associates, LLC under Contract No. DE-AC05-06OR23177 with the U.S. Department of Energy.
†bogacz@jlab.org

Content from this work may be used under the terms of the CC BY 3.0 licence (© 2019). Any distribution of this work must maintain attribution to the author(s), title of the work, publisher, and DOI

ISBN: 978-3-95450-217-2 doi:10.18429/JACoW-ERL2019-TUCOXBS04

energy, it is crucial to minimize the emittance dilution; therefore, the cells are tuned to minimize the dispersion in the bending sections, as in a theoretical minimum emittance lattice. At the lowest energy, it is possible to compensate for the bunch elongation with a negative momentum compaction setup which, additionally, contains the beam size. The intermediate energy arcs are tuned to a double bend achromat (DBA)-like lattice, offering a compromise between isochronicity and emittance dilution. Figure 3 illustrates all three settings of the arc cells. Tapering will be required in particular for Arc 6, where the beam loses more than 1% of its total energy.

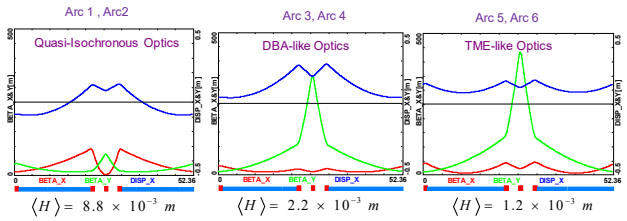

Figure 3: Different tunings of the arc cells at different energies. From left to right: low energy quasi-isochronous, middle energy DBA-like, high energy TME-like.

Before and after each arc a matching section adjusts the optics from and to the linac. Adjacent to these, additional cells additional cells are placed, hosting the RF compensating sections. The compensation makes use of a second harmonic field to replenish the energy lost by synchrotron radiation for both the accelerating and the decelerating beam, therefore allowing them to have the same energy at the entrance of each arc.

Path length-adjusting chicanes were also foreseen to tune the beam time of flight in order to hit the proper phase at each linac injection. Later investigations proved them to be effective only with the lowest energy beam, as these chicanes triggers unbearable energy losses if applied to the higher energy beams. A possible solution may consist in distributing the perturbation along the whole arc with small orbit excitations.

An alternative design based on FFA (Fixed Field Alternating Gradient) have been proposed and explored. It allows one to transport multiple energies in the same beam pipe, although only a very specific energy is bent with a constant radius. A drop-in FFA arc tuned to the 60 GeV energy showed promising results when substituted in the lattice, mainly because of the much higher bending filling factor, which mitigates synchrotron radiation. Nevertheless the LHeC would still need at least two FFA arcs on each side and it is not yet clear if the benefits compensate for the added complexity.

Spreaders and Recombiners

The spreaders are placed after each linac, and they separate bunches at different energies in order to route them to the corresponding arcs. The recombiners do just the opposite, merging the beams into the same trajectory before entering the next linac.

The spreader design consists of a vertical bending magnet, common for all beams, that initiates the separation. The highest energy, at the bottom, is brought back to the horizontal plane with a chicane, as illustrated in Fig. 4. The lower energies are captured with a two-step vertical bending adapted from the CEBAF design [5].

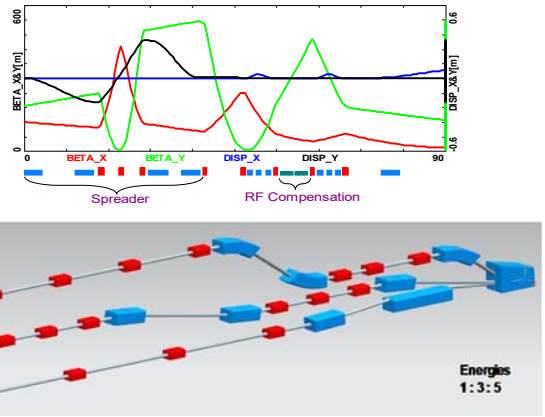

Figure 4: Spr/Rec Optics (top) and configuration (bottom)

The Bypass

While after the last spreader the 60 GeV beam can go straight to the interaction region, the lower energies beams, at 20 and 40 GeV, needs to be further separated in order to avoid interference with the detector. Different design options for the bypass section were explored and the one that minimizes the extra bending has been chosen and installed in the lattice.

Ten arc-like dipoles are placed very close to the spreader, to provide an initial bending, which results in 10 m separation from the detector located 150 m downstream. The straight section of the bypass is approximately 300 m long. In order to join the footprint of Arc 6, 10 of the 60 standard cells in Arc 2 and Arc 4 are replaced with seven higher field cells. The number of junction cells is a compromise between the field strength increase and the length of additional bypass tunnel, as can be inferred from the scheme in Fig. 5.

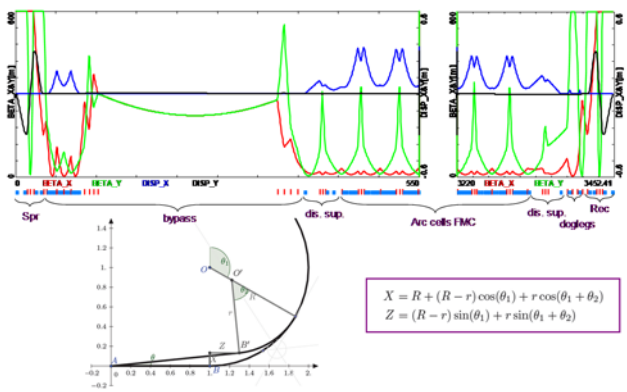

Figure 5: Layout of the bypass and optics. Featuring: the matching section from the linac, the initial bending, the long straight, the dispersion suppressor, cells with higher bending field and regular arc cells.

The stronger bending in the junction cells creates a small mismatch which is corrected by adjusting the strengths of

Content from this work may be used under the terms of the CC BY 3.0 licence (© 2019). Any distribution of this work must maintain attribution to the author(s), title of the work, publisher, and DOI

ISBN: 978-3-95450-217-2 doi:10.18429/JACoW-ERL2019-TUCOXBS04

Content from this work may be used under the terms of the CC BY 3.0 licence (© 2019). Any distribution of this work must maintain attribution to the author(s), title of the work, publisher, and DOI

the quadrupoles in the last junction cell and in the first regular cell.

Synchrotron Radiation Effects

Scaling of energy recovery to multi-GeV energies also encounters incoherent synchrotron radiation energy loss and spread, which asymmetrize accelerated and decelerated beam energies and profiles. These asymmetries substantially complicate multi-pass energy recovery and matching, and ultimately they limit the energy reach of the ERL due to recirculating arc momentum acceptance.

Table 1 lists arc-by-arc dilution of the longitudinal and transverse emittances due to quantum excitations. High luminosity colder requirements put very stringent limits on the allowed emittance increase. This can be met by design, employing low emittance optics arcs implemented in our design.

Table 1: Emittance Dillution Due to Synchrotron Radiation

Arc #	E [GeV]	ΔE [MeV]	$\Delta\varepsilon_n^{\text{arc}}$ [m rad]	$\Delta\varepsilon_n$ [m rad]	$\Delta^{\text{arc}}\sigma_{\Delta E/E}$	$\Delta\ \sigma_{\Delta E/E}$
1	10.5	1	2.7e-9	2.7e-9	3.9e-6	3.9e-6
2	20.5	11	1.5e-7	1.5e-7	2.1e-5	2.4e-5
3	30.5	51	4.1e-7	5.6e-7	5.6e-5	8.0e-5
4	40.5	160	2.2e-6	2.8e-6	1.1e-4	1.9e-4
5	50.5	387	4.6e-6	7.4e-6	2.0e-4	3.9e-4
6	60.5	797	1.4e-5	2.1e-5	3.1e-4	7.0e-4
5	50.5	387	4.6e-5	2.5e-5	2.0e-4	8.9e-4
4	40.5	160	2.2e-5	2.8e-5	1.1e-4	1.0e-5
3	30.5	51	4.1e-7	2.81e-5	5.6e-5	1.06e-5
2	20.5	11	1.5e-7	2.82e-5	2.1e-5	1.08e-5
1	10.5	1	2.7e-9	2.825e-5	3.9e-6	1.09e-5
Dump	0.5			2.825e-5		1.09e-5

'DOGBONE' TOPOLOGY ERL

So far, we have considered a 'Racetrack' configuration for an ERL. However, there are certain advantages of an alternative 'Dogbone' topology, which was first considered for rapid acceleration of fast decaying muons, as part of Neutrino Factory design [6]. Here, we propose a multi-pass electron ERL consisting of a single superconducting linac configured with elliptical twin axis cavities [7], capable of accelerating (or decelerating) beams in two separate beam pipes (see Fig. 6a). Such cavity, features opposite direction longitudinal electric fields in the two halves of the cavity, as illustrated schematically in Fig. 6b.

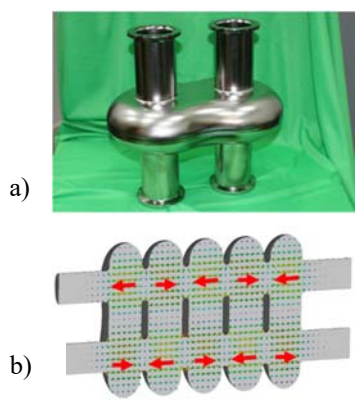

Figure 6: Elliptical twin axis cavity: a) Single cell Niobium cavity; b) Configuration of electric fields with opposing directions in two halves of a multi-cell cavity.

As illustrated in Fig. 7, the beam is injected via a fixed field chicane at the middle of the linac to minimize the effect of phase slippage for the lowest energy beam accelerated in the linac, which is phased for the speed-of-light particle. At the linac ends the beams need to be directed into the appropriate energy-dependent (pass-dependent) 'droplet' arc for further recirculation [8] (a pair of droplet arcs at each end of the linac). Reusing the same linac for multiple (3.5) beam passes provides for a more compact and efficient accelerator design and leads to significant cost savings [9]. Furthermore, this scheme is well suited to operate in the energy recovery mode.

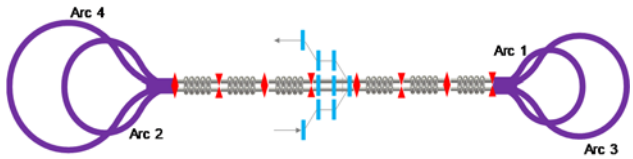

Figure 7: Multi-pass 'Dogbone' ERL – Schematic view of the accelerator layout; featuring a single SRF linac based on elliptical twin axis cavities, four return 'droplet' arcs and a pair of injection/extraction chicanes.

Multi-pass Linac

The focusing profile along the linac was chosen so that energy recovered beams with a large energy spread could be transported within the given aperture. Since the beam is traversing the linac in both directions (as being accelerated, or decelerated) two consecutive passes are accommodated in different 'halves' of elliptical twin axis cavities. To assure adequate focusing for counter propagating beams a 'bisected' focusing profile was chosen for the multi-pass linac [10]. Here, the quadrupole gradients were set to scale up with momentum to maintain 90° phase advance per cell for the first half of the linac and then they were mirror reflected in the second half to mitigate the beta beating resulting from under-focusing for the first full pass through the linac, as illustrated in Fig. 8. Multi-pass linac optics for all 3.5 passes is illustrated in Fig. 9.

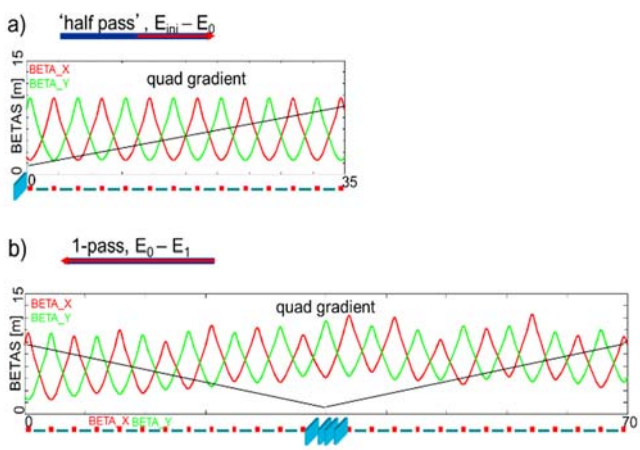

Figure 8: "Bisected" linac optics: (a) periodic FODO structure set for the lowest energy 'half-pass' through the linac; (b) linac optics for the first 'full pass'; the under focusing

ISBN: 978-3-95450-217-2 doi:10.18429/JACoW-ERL2019-TUCOXBS04

effects in the first half of the linac are mitigated by reversing the focusing profile in the second half.

One can notice the 'bisected' linac optics naturally supports energy recovery, providing an extra path length delay of one half of the RF wavelength is added to the highest energy arc (Arc 4), which will put the beam into a decelerating mode. The linac optics for 3.5 decelerating passes (energy recovery) follows a mirror symmetric optics to the one illustrated in Fig. 9.

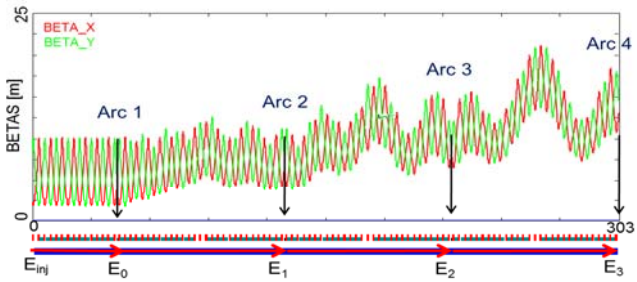

Figure 9: Multi-pass linac optics for all passes, with mirror symmetric arcs inserted as point matrices (arrows). The virtue of the optics is the appearance of distinct nodes in the beta beat-wave at the ends of each pass (where the arcs begin), which limits the growth of initial betas at the beginning of each subsequent droplet arc (Arc 1–4), hence eases linac-to-arc matching.

'Droplet' Arcs

At the ends of the RLA linac, the beams need to be directed into the appropriate energy-dependent (pass-dependent) droplet arc for recirculation. The entire droplet-arc architecture [8] is based on 90° phase-advance cells with periodic beta functions. For practical reasons, horizontal rather than vertical beam separation has been chosen. Rather than suppressing the horizontal dispersion created by the spreader, it has been matched to that of the outward arc. This is partially accomplished by removing one dipole (the one furthest from the spreader) from each of the two cells following the spreader. To switch from outward to inward bending, three transition cells are used, wherein the four central dipoles are removed. The two remaining dipoles at the ends bend the same direction as the dipoles to which they are closest. The transition region, across which the horizontal dispersion switches sign, is therefore composed of two such cells. To facilitate subsequent energy recovery following acceleration, a mirror symmetry is imposed on the droplet arc optics. This puts a constraint on the exit/entrance Twiss functions for two consecutive linac passes, namely: $\beta_{n\,out} = \beta_{n+1\,in}$ and $\alpha_{n\,out} = -\alpha_{n+1\,in}$, where n = 0, 1, 2... is the pass index.

The complete droplet arc optics for the lowest-energy pair of arcs is shown in Fig. 10. All higher arcs are based on the same principle as Arc 1, with gradually increasing cell length (and dipole magnet length) to match naturally to the increasing beta functions dictated by the multi-pass linac. The quadrupole strengths in the higher arcs are scaled up linearly with momentum to preserve the 90° FODO lattice. The physical layout of the above pair of droplet arcs is illustrated in Fig. 11.

One additional requirement to support energy recovery in a linac configured with elliptical twin axis cavities is that the path-length of Arcs 1-3 has to be a multiple of the RF wavelength. Conversely, Arc 4 path-length should be a multiple plus one half of the RF wavelength to switch the beam from the 'accelerating' to 'decelerating' phase in the linac.

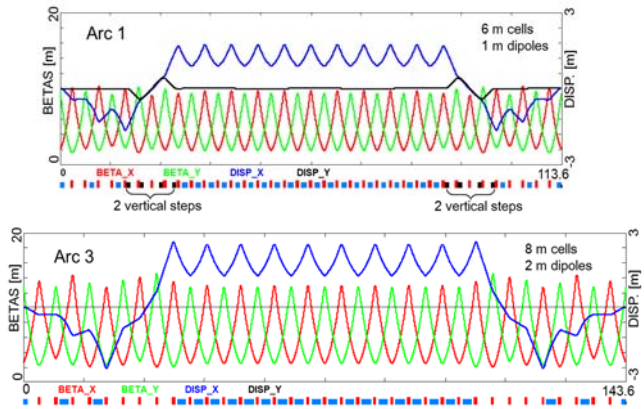

Figure 10: 'Droplet' arc optics for a pair of arcs on one side of the 'Dogbone'; Arc 1 and Arc 3.

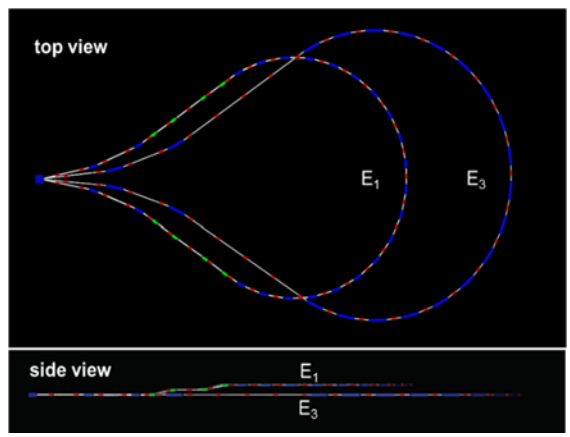

Figure 11: Layout of a pair of arcs on one side of the 'Dogbone' RLA, Top and side views, showing vertical two-step 'lift' of the middle part of lower energy droplet arc to avoid interference with the larger droplet (1 meter vertical separation).

OUTLOOK

The maximum number of passes through the RLA's linac is often limited by design considerations for the switchyard, which first spreads the different energy passes to go into the appropriate arcs and then recombines them to align the beam with the linac axis. To reduce complexity of the above single energy return arcs, we have recently proposed a novel multi-pass arc design based on linear combined function magnets with variable dipole and quadrupole field components, which allows two consecutive

Content from this work may be used under the terms of the CC BY 3.0 licence (© 2019). Any distribution of this work must maintain attribution to the author(s), title of the work, publisher, and DOI

ISBN: 978-3-95450-217-2 doi:10.18429/JACoW-ERL2019-TUCOXBS04

Content from this work may be used under the terms of the CC BY 3.0 licence (© 2019). Any distribution of this work must maintain attribution to the author(s), title of the work, publisher, and DOI

passes with very different energies (factor of two, or more) to be transported through the same string of magnets [11]. Such a solution combines compactness of design with all the advantages of a linear, non-scaling FFA (Fixed Field Alternated Gradient) optics [12], namely, large dynamic aperture and momentum acceptance essential for energy recovery, no need for complicated compensation of non-linear effects, and one can use a simpler combined-function magnet design with only dipole and quadrupole field components. The scheme utilizes only fixed magnetic fields, including those for injection and extraction.

SUMMARY

Here, we discussed novel approach to meet the LHeC challenges of adding new accelerator capabilities (ERL with multiple-passes, tens of GeV at high current, tens of mA). They were addressed through exploration of innovative lattice solutions. Effective implementation of Energy Recovering Linac technology requires: proper design of multi-pass optics, fine control of beam stability and losses (halo), preservation of 6D bunch quality, energy recovery efficiency, multiple-beam diagnostic devices, and development of ERL-specific commissioning and optics tuning procedures[13], [14].

Presented unique design of the IR optics gives the impression that luminosity of 10^{34} $cm^{-2}s^{-1}$ is within reach.

The key advantage of a multi-pass RLA is its very efficient use of an expensive SRF linac. That efficiency can be further enhanced by configuring an RLA in a 'Dogbone' topology, which almost doubles the RF efficiency (compare to a corresponding racetrack). Furthermore, the 'Dogbone' RLA is well suited for operation in the energy recovery mode. Finally, we have presented a-proof-of-principle lattice design of a multi-pass energy recovery linac (ERL) in a 'Dogbone' topology.

REFERENCES

[1] D. Pellegrini, A. Latina, D. Schulte and S.A. Bogacz, "Beam-dynamics Driven Design of the LHeC Energy Recovery Linac", *Phys. Rev. ST-AB*, 121004 (2015). doi:10.1103/PhysRevSTAB.18.121004

[2] D. Pellegrini, "Beam Dynamics Studies in Recirculating Machines", Ph.D. Thesis, EPFL, Switzerland, 2016.

[3] O. Brüning *et al,* "Development of an ERL Based TeV Energy ep and eA Collider at CERN" *ICFA Beam Dynamics Newsletter* No 68, December 2015.

[4] J. Rosenzweig and L. Serafini, "Transverse particle motion in radio-frequency linear accelerators", *Phys. Rev. E*, vol. 49, Feb 1994. doi:10.1103/PhysRevE.49.1599

[5] "12 GeV CEBAF Upgrade", Reference Design, www.jlab.org/12GeV

[6] S.A. Bogacz, "Beam Dynamics of Muon Acceleration for Neutrino Factory', *Journal of Physics G: Nuclear and Particle Physics*, 29, 1723 (2003). doi:10.1088/0954-3899/29/8/338

[7] H. Park, S. U. De Silva, J. R. Delayen, F. Marhauser, A. Hutton, 'First Test Results of Superconducting Twin Axis Cavity for ERL Applications', *Proceedings of LINAC 2018*, Beijing, China (2018). doi:10.18429/JACoW-LINAC2018-TUPO032

[8] C. Ankenbrandt *et al.*, "Low Energy Neutrino Factory Design", Phys. Rev. ST-AB **12**, 070101 (2009). doi:10.1103/PhysRevSTAB.12.070101

[9] J.S. Berg *et al.*, "Cost-effective Design for a Neutrino Factory", *Phys. Rev. ST-AB* **9**, 011001(2006). doi:10.1103/PhysRevSTAB.9.011001

[10] S.A. Bogacz, "Muon Acceleration Concepts for NuMAX: 'Dual-use' Linac and 'Dogbone' RLA", *JINST*, 13, P02002 (2018). doi:10.1088/1748-0221/13/02/P02002

[11] V.S. Morozov, S.A Bogacz, Y.R. Roblin, K.B. Beard, "Linear Fixed-field Multi-pass Arcs for Recirculating Linear" *PRST-AB*,**15**, 060101 (2012). doi: 10.1103/PhysRevSTAB.15.060101

[12] V.S. Morozov, S.A Bogacz, K.B. Beard, "Muon Acceleration with RLA and Non-scaling FFA Arcs", in *Proc. IPAC'10*, Kyoto, Japan (2010). Paper: WEPE084

[13] A.B. Temnykh, "Beam Losses Due to Intra-Beam and Residual Gas Scattering for Cornell's Energy Recovery Linac", in *Proc. EPAC08*, MOPC064, pp. 214-216, Genoa, Italy (2008).

[14] P. Evtushenko, "Large Dynamic Range Beam Diagnostics for High Average Current Electron Linacs", in *Proc. IPAC2014*, WEYB01, pp. 1900-1905, Dresden, Germany, (2014). doi:10.18429/JACoW-IPAC2014-WEYB01